# Background Control and Upper Limit on the Chiral Magnetic Effect in Isobar Collisions at $\sqrt{s_{\text{NN}}} = 200$ GeV from STAR

*Yicheng* Feng[1,*] for the STAR Collaboration

[1]Department of Physics and Astronomy, Purdue University, West Lafayette, IN 47907

**Abstract.** The STAR Collaboration has reported results from a blind analysis of isobar collisions ($^{96}_{44}$Ru + $^{96}_{44}$Ru, $^{96}_{40}$Zr + $^{96}_{40}$Zr) at $\sqrt{s_{\text{NN}}} = 200$ GeV on the search for the chiral magnetic effect (CME). Significant differences were observed in the measured multiplicity ($N$) and elliptic anisotropy ($v_2$) between the two isobar systems. In these proceedings, we present two post-blind analyses aimed at mitigating remaining background effects. The first involves employing an event weighting procedure to match the distributions in $N$ and $v_2$ and then compare the CME-sensitive $\Delta\gamma$ correlator and signed balance functions. The second analysis investigates the contributions of the two- and three-particle nonflow to the isobar ratio of $\Delta\gamma/v_2$. The estimated background baseline is consistent with the isobar measurements, and an upper limit is extracted on the CME signal.

## 1 Introduction

The chiral magnetic effect (CME) is a charge separation phenomenon, induced by chirality imbalance of quarks in heavy-ion collisions under a strong magnetic field produced by spectator protons [1]. This chirality imbalance can be caused by nonzero topological charge in a local domain because of vacuum fluctuations in quantum chromodynamics (QCD). A strong magnetic field can be produced in non-central heavy-ion collisions by spectator protons. The charge separation is then induced by the charge-dependent magnetic moments of the excess quarks of one chirality.

To search for the CME, isobar $^{96}_{44}$Ru + $^{96}_{44}$Ru and $^{96}_{40}$Zr + $^{96}_{40}$Zr collisions at $\sqrt{s_{\text{NN}}} = 200$ GeV were conducted in 2018 by STAR [2]. The two isobar species were expected to have similar backgrounds because of the same nucleon number, whereas the CME signal is expected to be larger in the former because of the stronger magnetic field produced by the more spectator protons [3]. However, data indicate different measured multiplicity ($N$) and elliptic flow ($v_2$) between the two isobar systems [4]. Such differences had been predicted to result from variations in the nuclear structures of the isobars [5]. As a result, the isobar ratio (Ru+Ru/Zr+Zr) of the CME-sensitive observable of the $v_2$-scaled charge separation ($\Delta\gamma/v_2$) is below unity, contrary to the initial expectation. Because the background is proportional to elliptic flow over multiplicity, $\Delta\gamma \propto v_2/N$, the expected baseline for the $\Delta\gamma/v_2$ isobar ratio is the inverse multiplicity ($1/N$) ratio. However, the measured data is systematically larger. This could indicate the potential existence of a CME signal [6]. This could also indicate the presence of additional background different between the isobars [7]. Besides the $1/N$ ratio,
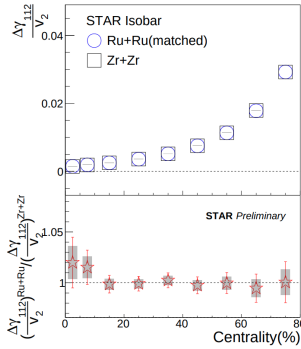
---

**Figure 1.** The $\Delta\gamma/v_2$ of Ru+Ru, Zr+Zr, and Ru+Ru/Zr+Zr as functions of centrality at $\sqrt{s_{NN}} = 200$ GeV. The multiplicity distribution of Ru+Ru collisions has been weighted to match to that of Zr+Zr.
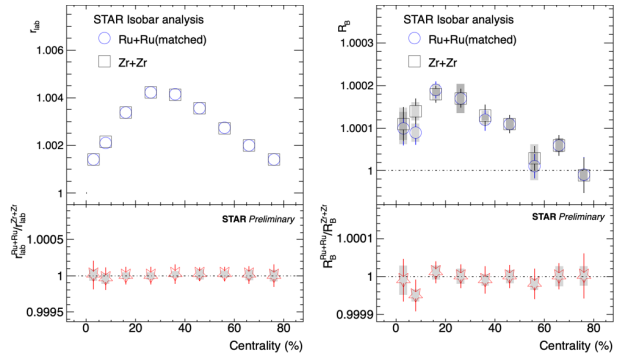
**Figure 2.** The SBF's, $r_{lab}$ and $R_B$, for Ru+Ru, Zr+Zr, and Ru+Ru/Zr+Zr as functions of centrality at $\sqrt{s_{NN}} = 200$ GeV. The multiplicity, observed $v_2$, and EP resolution distributions of Ru+Ru collisions have all been matched to those of Zr+Zr simultaneously.

another viable expectation of the baseline is the pair multiplicity ratio, which is generally higher than the $\Delta\gamma/v_2$ isobar ratio [4].

To understand ~~those~~ these observations, two post-blind analyses have been carried out. One is the forced-match analysis, which re-weights the events according to $N$, observed $v_2$, and event plane (EP) resolution to mitigate the isobar differences. In the other analysis, various nonflow backgrounds are estimated for the isobar ratio of $\Delta\gamma/v_2$ to extract a rigorous background baseline [7]. These proceedings report the findings from the two analyses.

## 2 Forced match analysis

The events in a given narrow centrality ~~bin~~ class can be categorized into bins in $N$, observed $v_2$, and EP resolution. In each bin, the ratio of the number of Zr+Zr events over that of Ru+Ru is defined as a weight factor, called $f_{W,bin}$. The observables in Ru+Ru are then weighted by $f_{W,bin}$ before comparison to those directly measured in Zr+Zr.

First, we apply $f_{W,bin}(N)$ to match the multiplicities between the two isobars and calculate $v_2$ and $\Delta\gamma$. Figure 1 shows $\Delta\gamma/v_2$ for Ru+Ru, Zr+Zr, and the Ru+Ru/Zr+Zr ratio after this multiplicity matching. The ratio is consistent with unity (Fig. 1 lower panel), indicating no observed signal. ~~We then~~ Then we match all the three quantities by applying $f_{W,bin}(N, v_2, \text{EP resolution})$ for the signed bal-



**Figure 3.** The 20-50% centrality averages of the isobar ratios of $\Delta\gamma/v_2$, $r_{lab}$, and $R_B$ with Ru+Ru weighted to match to Zr+Zr.

ance functions (SBF)~~, which examine~~: $r_{lab}$, $R_B$ [8]. The SBF examines the fluctuation of net momentum-ordering of charged pairs~~so as~~, allowing us to study the charge separation
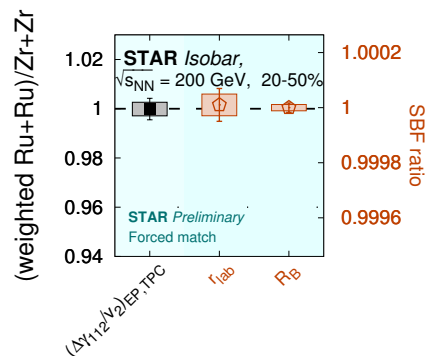
induced by the CME [8, 9]. Figure 2 shows that the isobar ratios of both SBF's are consistent with unity, again indicating no observed signal. Figure 3 summarizes the results from the forced match analysis for mid-central collisions.

## 3  Background baseline analysis and CME upper limit

The $\Delta\gamma$ is often measured by 3-particle azimuthal correlations [10]:

$$C_{3,\alpha\beta} = \langle\cos(\phi_\alpha + \phi_\beta - 2\phi_c)\rangle, \quad \gamma_{\alpha\beta} = C_{3,\alpha\beta}/v_2^*, \quad \Delta\gamma = \gamma_{os} - \gamma_{ss}. \tag{1}$$

The average is taken over all triplets in an event and over all events, where indices $\alpha$, $\beta$ stand for a pair of particles of interest (POI), $c$ is a third particle for EP reference, whose resolution equals to $v_2^*$ [10], and the subscript OS means opposite-sign charged pair of $(\alpha, \beta)$ and SS same-sign. The asterisk on $v_2^*$ denotes an inclusive anisotropy measurement including nonflow, $v_2^* = \sqrt{\langle\cos 2(\phi_\alpha - \phi_\beta)\rangle}$. The *true* elliptic flow is denoted by $v_2$, and the nonflow fraction in $v_2^*$ measurement is $\epsilon_{nf} = (v_2^{*2} - v_2^2)/v_2^2$. The backgrounds in $\Delta\gamma$ can be decomposed into [7]

$$\frac{\Delta\gamma_{bkgd}}{v_2^*} = \frac{C_3}{v_2^{*2}} = \frac{C_{2p}}{N}\frac{v_2^2}{v_2^{*2}} + \frac{C_{3p}}{N^2 v_2^{*2}} = \frac{C_{2p}v_2^2}{N v_2^{*2}}\left(1 + \frac{C_{3p}/C_{2p}}{N v_2^2}\right), \tag{2}$$

where $N$ is the number of POI. The $C_{2p}$ is defined as $C_{2p} = Nr(C_{2p,os}v_{2,2p}/v_2 - \gamma_{ss}/v_2)$, where $C_{2p,os} = \langle\cos(\phi_\alpha^\pm + \phi_\beta^\mp - 2\phi_{2p})\rangle_{2p}$ is calculated over the correlated pairs (2p), and $v_{2,2p}$ is the elliptic flow of the pair. The $r$ is the relative pair excess of OS over SS pairs, $r = N_{2p}/N_{os} = (N_{os} - N_{ss})/N_{os}$ [7]. The $C_{3p}$ is defined as $C_{3p} = N(C_{3p,os}N_{3p,os}/N_{os} - C_{3p,ss}N_{3p,ss}/N_{ss})$, where $C_{3p,\alpha\beta} = \langle\cos(\phi_\alpha + \phi_\beta - 2\phi_c)\rangle_{3p}$ are calculated over the correlated triplets (3p), and $N_{3p,\alpha\beta}$ are their numbers [7]. The isobar ratio is then given by [7, 11]

$$\frac{\left(\Delta\gamma_{bkgd}/v_2^*\right)^{Ru}}{\left(\Delta\gamma_{bkgd}/v_2^*\right)^{Zr}} \approx 1 + \frac{\delta(C_{2p}/N)}{C_{2p}/N} - \frac{\delta\epsilon_{nf}}{1+\epsilon_{nf}} + \frac{1}{1 + \frac{N v_2^2}{C_{3p}/C_{2p}}}\left(\frac{\delta C_{3p}}{C_{3p}} - \frac{\delta C_{2p}}{C_{2p}} - \frac{\delta N}{N} - \frac{\delta v_2^2}{v_2^2}\right). \tag{3}$$

Three contributions to the background:

(1) The first term is the widely-studied flow-induced 2p background, e.g., resonance decay daughter pairs coupled with the elliptic flow of the resonance. The 2p nonflow $C_{2p}/N$ is proportional to $r$ and decay kinematics of the pair. The two isobars should be highly similar in those decay kinematics, so the difference in relative pair multiplicity can be used to estimate the difference in 2p nonflow [7]. The systematic uncertainty is assessed by various pair mass ranges in obtaining $r$.

(2) The second term is due to the nonflow in $v_2^*$. ~~The SS pair ($\Delta\eta$, $\Delta\phi$)~~ The 2D ~~distributions~~ ($\Delta\eta$, $\Delta\phi$) distributions of SS pair are fitted to separate nonflow from flow~~, where~~. Here nonflow is modeled ~~by~~ using 2D Gaussians~~and~~, while flow is modeled ~~by~~ using a Fourier series independent of $\Delta\eta$ ~~-independent Fourier series~~. We take an alternative fit function and the measured flow decorrelation for estimation of systematic uncertainties. ~~The systematic uncertainties are assessed by alternative fit function and the measured flow decorrelation.~~

(3) The third term is the 3p nonflow, where all the three particles are correlated, ~~like in jets. We use~~ such as jets. We employ the HIJING simulation to estimate ~~it.~~ this term. Since HIJING does not have flow, the inclusive $C_3$ ~~in HIJING all comes~~ originates solely from 3p nonflow correlations, denoted as $C_{3p}$. ~~The default HIJING simulation includes~~ The standard HIJING simulation accounts for jet quenching, ~~and that~~ while the version without jet quenching is ~~taken for systematics~~ used for systematic analysis.

Figure 4 shows the background baseline of Eq. 3 for full events (left), and subevents (right) as functions of centrality. The background baselines are calculated for four measurements using cumulant method, and the 20-50% centrality average of baselines are shown by brown bands in Fig. 5 together with the data measurements in the blind analysis [4]. ~~They are all consistent with the data measurements~~The above background baseline estimates are in agreement with the observed data from isobar blind analysis. Assuming 15% CME signal difference between the isobars [10, 12], upper limits ~~are extracted on~~ of the CME fraction ($f_{CME}$~~in the four~~) are derived for the four types of $\Delta\gamma$ ~~measurements~~observables. The upper limits are around 10% at 95% confidence level.
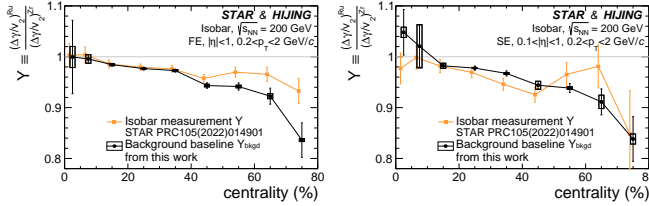


**Figure 4.** The measurements [4] and background baseline [7], the isobar ratio of $\Delta\gamma/v_2$, as functions of centrality from full events (left) and subevents (right).
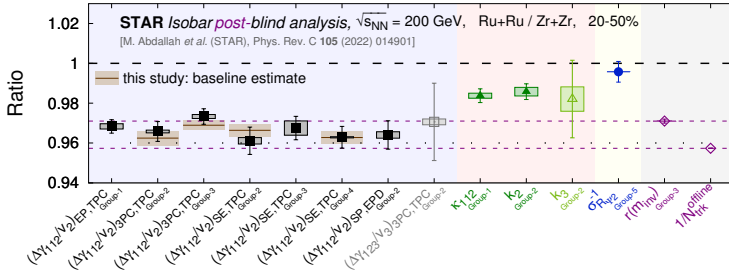


**Figure 5.** The background baseline estimates [7] for the four cumulant measurements, together with the isobar ratio measurements of $\Delta\gamma/v_2$ in 20-50% centrality from the STAR blind analyses [4], .

## 4 Summary

Isobar Ru+Ru and Zr+Zr collisions are conducted to search for the CME with expectation of equal background and different signals. The isobar blind analysis by STAR [4] showed that the isobar collision systems differ in multiplicity $N$ and elliptic flow $v_2$ and hence also in CME backgrounds. Scaling the number of Ru+Ru events to that of Zr+Zr in bins of $N$, observed $v_2$, and EP resolution, the isobar ratios are consistent with unity and indicate non-observable CME signal. The background baseline is estimated accounting for 2p and 3p nonflow contamination in addition to the flow-induced background and found to be consistent with the measured $\Delta\gamma/v_2$ isobar ratio data. An upper limit of around 10% on the CME fraction in $\Delta\gamma$ is extracted with 95% confidence level.

## References

[1] D. E. Kharzeev, L. D. McLerran and H. J. Warringa, Nucl. Phys. A **803**, 227-253 (2008).

[2] V. Koch, *et al.* Chin. Phys. C **41**, no.7, 072001 (2017).

[3]  S. A. Voloshin, Phys. Rev. Lett. **105**, 172301 (2010).

[4]  STAR Collaboration, Phys. Rev. C **105**, no.1, 014901 (2022).

[5]  H. J. Xu *et al.* Phys. Rev. Lett. **121**, no.2, 022301 (2018).

[6]  D. E. Kharzeev, J. Liao and S. Shi, Phys. Rev. C **106**, no.5, L051903 (2022).

[7]  STAR Collaboration, arXiv:2308.16846 [nucl-ex].

[8]  A. H. Tang, Chin. Phys. C **44**, no.5, 054101 (2020).

[9]  S. Choudhury *et al.* Chin. Phys. C **46**, no.1, 014101 (2022).

[10]  S. A. Voloshin, Phys. Rev. C **70**, 057901 (2004).

[11]  Y. Feng, J. Zhao, H. Li, H. j. Xu and F. Wang, Phys. Rev. C **105**, no.2, 024913 (2022).

[12]  W. T. Deng, X. G. Huang, G. L. Ma and G. Wang, Phys. Rev. C **94**, 041901 (2016).